S30. CONTRIBUTORS TO THE RECORD HIGH TEMPERATURES ACROSS AUSTRALIA IN LATE SPRING 2014

Pandora Hope, Eun-Pa Lim, Guomin Wang, Harry H. Hendon, and Julie M. Arblaster

This document is a supplement to "Contributors to the Record High Temperatures Across Australia in Late Spring 2014," by Pandora Hope, Eun-Pa Lim, Guomin Wang, Harry H. Hendon, and Julie M. Arblaster (*Bull. Amer. Meteor. Soc.*, **96** (12), S149–S153) • DOI:10.1175/BAMS-D-15-00096.1

Data. Monthly maximum temperatures from the Australian Water Availability Project (AWAP) gridded dataset (Jones et al. 2009) were analyzed on a 0.25° grid over Australian land points. Observed sea surface temperatures from Hurrell et al. (2008) for 1981 and Reynolds et al. (2002) from 1982 onwards were used for the ENSO index (based on Niño-3.4 SSTs: 5°N–5°S, 170°–120°W) and the Indian Ocean dipole mode index [IOD: western pole (10°S–10°N, 50°–70°E); eastern pole (10°S–0°, 90°–110°E); Saji et al. 1999]. The SAM was calculated as the first EOF of mean sea level pressure (MSLP) anomalies over 20°–75°S (e.g., Lim et al. 2011) from the ERA-Interim reanalysis (Dee et al. 2011). Soil moisture estimates are from Raupach et al. (2009) for the upper-layer (<0.2m). Global mean temperatures were from the U.K. Met Office HadCRUT4 (version 4.3.0.0; www.metoffice.gov.uk/hadobs/hadcrut4/).

Experimental setup. The POAMA seasonal forecast system is a fully coupled atmosphere–land–ocean model used operationally at the Australian Bureau of Meteorology (Hudson et al. 2013). External anthropogenic and natural forcings are set to climatological values, though some of the impacts of long-term changes in these will be contained in the initial conditions. The Bureau's operational seasonal forecast for October and November was made up of 99 ensemble members (i.e., 11 perturbed initialization on 21, 25, and 28 September 2014 with 3 different model versions of POAMA; Cottrill et al. 2013). The CO_2 concentration used for the operational forecasts and hindcasts is fixed at 345 ppm, commensurate with levels in about 1985. The pdf of the ensemble members in the 2014 operational forecast is strongly shifted compared to the 1981–2010 hindcast climatology, indicating a 2.5-fold higher chance for unusual warm conditions to occur (Tmax > 1σ). The observed anomaly is captured within the ensemble spread, though at the outer edge of the range of forecasts.

The seasonal forecast control and experiments in this study use one version of POAMA (e24a), with 11 members, each initialized on 21, 25, and 28 September producing an ensemble of 33 members. The control experiment was initialized with observed atmosphere, ocean and land initial conditions generated from the BoM's data assimilation systems (Hudson et al. 2011; Yin et al. 2011) and the CO_2 concentration was set to 400 ppm, a level closer to those observed in 2014. The climatology used in Fig. 30.1 of main text is the hindcast climatology, with CO_2 concentrations set to 345 ppm. Considering only the model version used in the experiments (e24a), the hindcast climatology mean Tmax is 32.6°C and 1 standard deviation is 1.1°C.

In the first sensitivity experiment, the impact of running the model with a lower CO_2 concentration of 315 ppm, equivalent to 1960 levels is investigated. In this experiment, the ocean and atmosphere are initialized with September 2014 observed conditions. In the second sensitivity experiment, the model is again run with a CO_2 concentration of 315 ppm, but the ocean initial conditions are manipulated. In order

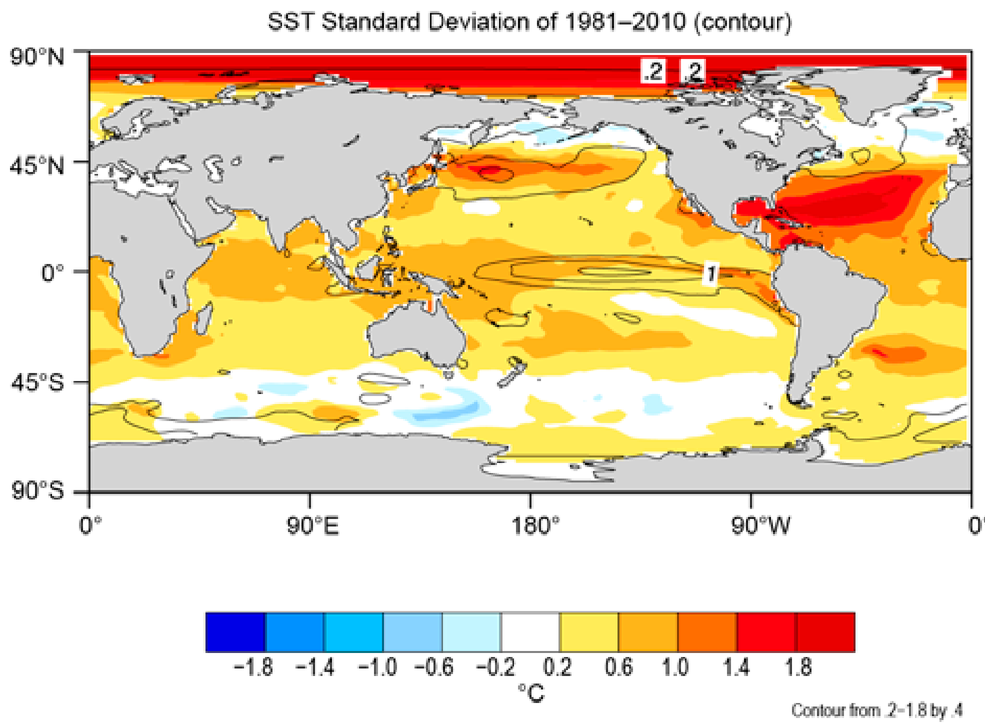

Fig. S30.1. Mean sea surface temperature difference (°C) between 2014 and 1960 as a result of prescribing observed changes in CO_2 over that period in the POAMA forecast model (see text for details). The standard deviation of monthly SSTs for the base period 1981–2010 is overlaid (contour interval 0.4°C) for reference.

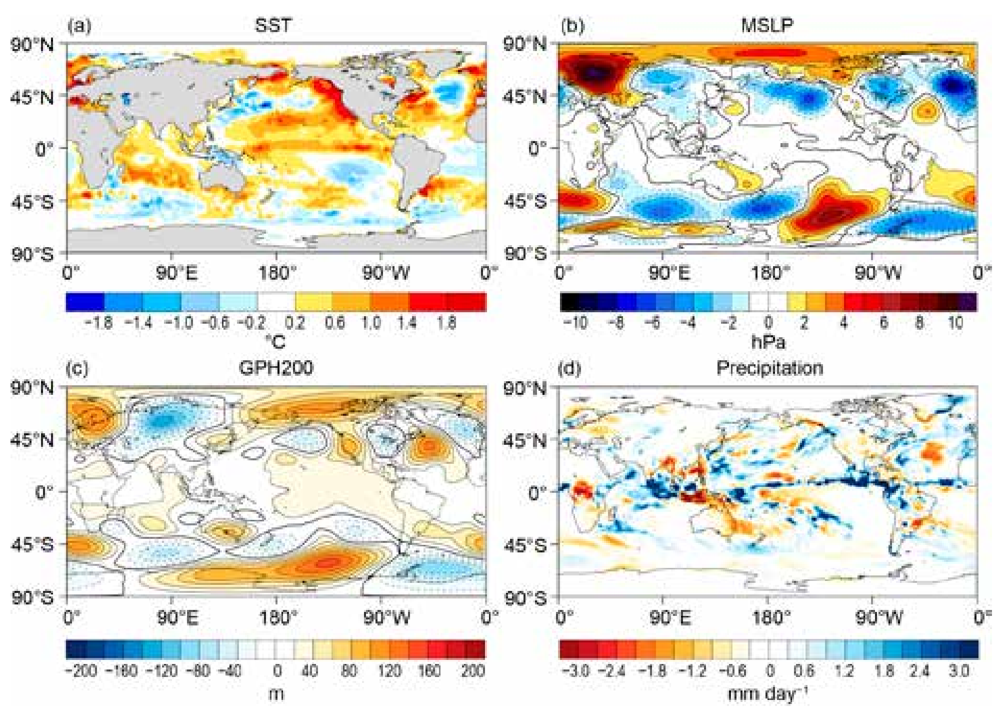

Fig. S30.2. Observed 2014 Oct–Nov mean anomalies of (a) SST (°C), (b) MSLP (hPa), (c) 200-hPa geopotential height (m) and (d) precipitation (mm day^{-1}) relative to the 1981–2010 climatology.

to remove the ocean's response to CO_2 over the last 50 years, an anomaly was removed from the initial conditions. The anomaly was created using free-running, coupled 30-year integrations of the seasonal forecast model with high (400 ppm, equivalent to 2014) or low (315 ppm, equivalent to 1960) CO_2 levels. No other radiative forcing agents were altered, in part due to the limited scope for altering such factors in the seasonal forecast model. To account for the decadally varying background state, two sets of observed initial conditions were used, a decade apart, for the recent conditions (2000 and 2010) and the 1960s conditions (1960 and 1970). Each of the four integrations was run for 30 years and an average from austral spring (September–November) of the last five years of each were used to create an estimate of the global warming in the oceans due to CO_2 increase since 1960, termed 'oceanCO_2anom' (Fig. S30.1). The anomalous temperature and salinity were removed from the full 2014 ocean to initialize the experiment. This experiment was termed 'preCO_2'.

Although POAMA suffers from a cold mean state bias when run in climate mode (e.g., Lim et al. 2010) and was only forced with varying CO_2, the pattern of surface temperature change is similar to the CMIP5 mean modelled trend over the historical period (Bindoff et al. 2013), with warming near the equator across the Pacific Ocean and in the north of each ocean basin. The similarity between the CMIP5 trend and the POAMA anomaly suggests that the influence from other radiative forcings such as aerosols or the ozone hole were small. While recent studies have suggested that ozone concentrations over Antarctica may influence year-to-year fluctuations in Australian temperatures in October (Son et al. 2013) and austral summer (Bandoro et al. 2014) by driving changes in the SAM, they do not appear relevant to late spring 2014 (given the minimal role of the SAM; see Fig. S30.2). The pattern of sub-surface change in POAMA from the top 300 m (not shown) is similar to the results of 2×CO_2 experiments such as DiNezio et al. (2012). The difference created with POAMA forced with two levels of CO_2 was deemed preferable to the CMIP5 multimodel derived warming since the initial conditions for the subsequent forecasts would be in internal dynamical balance and potential errors from extensive interpolation required over multiple models, particularly across varying bathymetry, would be avoided.

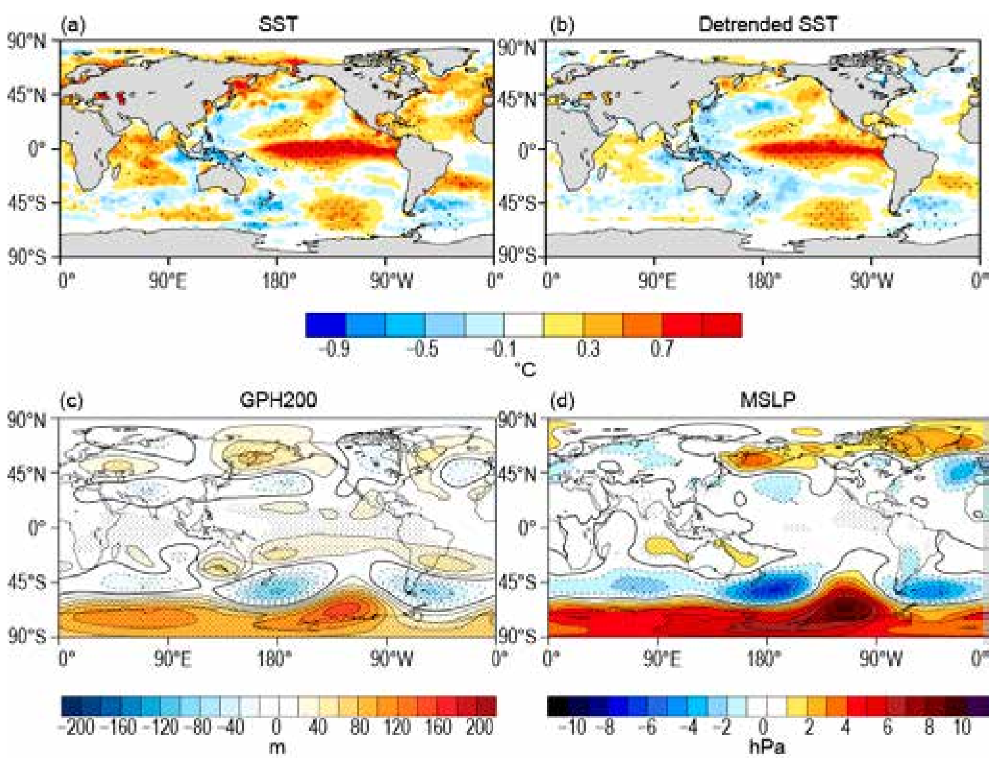

Fig. S30.3. Regression of Oct–Nov mean (a) SST (°C), (b) detrended SST (°C), (c) 200-hPa geopotential height (m) and (d) MSLP (hPa) anomalies on the standardized time series of Australian areal mean Tmax over the period 1981–2013. Regression coefficients were scaled by the magnitude of 2014 Oct–Nov mean Australian Tmax. Stippling indicates statistical significance at the 90% confidence level.

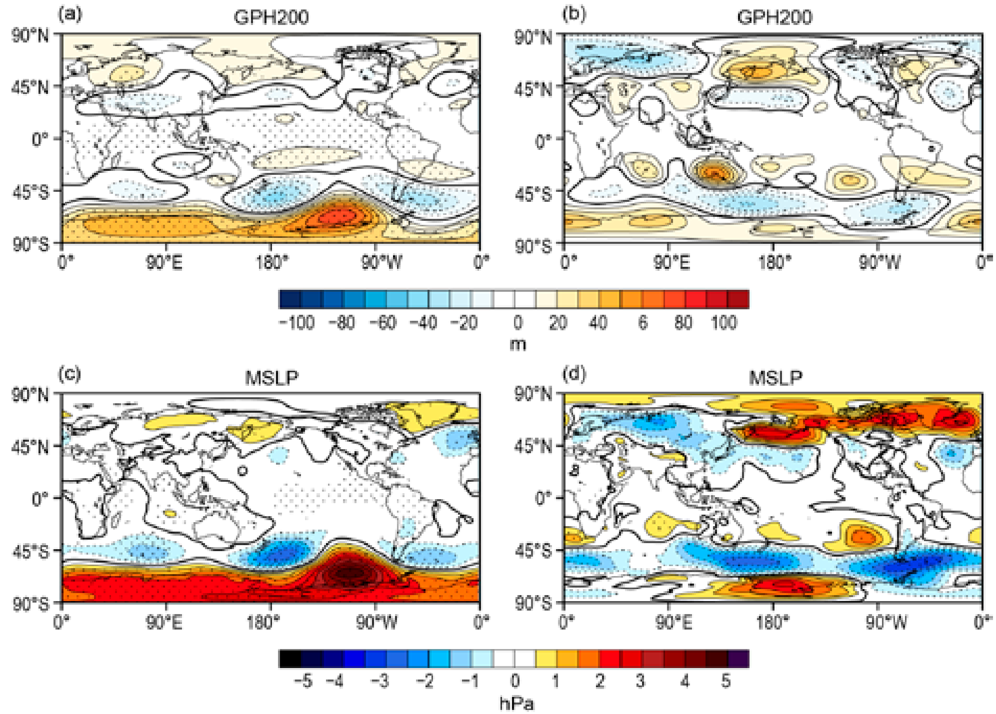

Fig. S30.4. Regression of (a),(b) 200-hPa level geopotential height (m) and (c),(d) MSLP (hPa) on the (a),(c) standardized reconstructed and (b),(d) residual time series of Australian Tmax obtained from the multiple linear regression described in the text and shown in Fig. 32.2m in main text. Regression coefficients were scaled by the magnitudes of the reconstructed and residual Tmax in 2014. Stippling indicates statistical significance at the 90% confidence level.

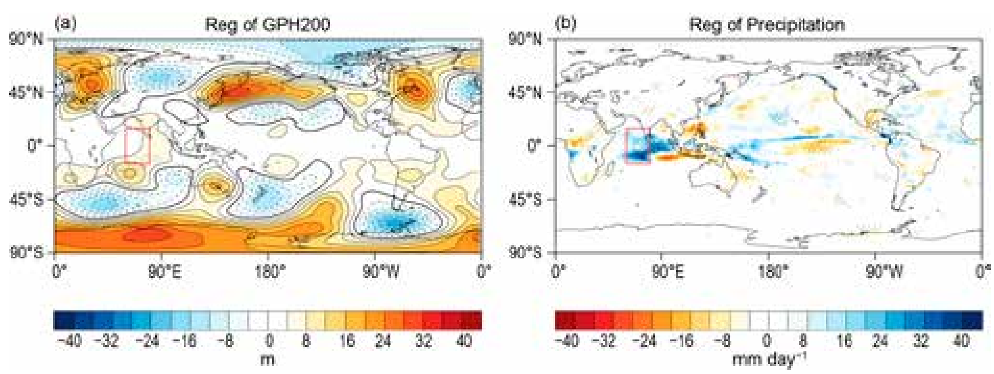

Fig. S30.5. Partial regression of (a) 200-hPa level geopotential height (m) and (b) precipitation anomaly (mm day-1) onto the rainfall index of tropical central Indian Ocean averaged over 15°S–15°N, 60°–80°E (red box), removing the influence of IOD. Stippling indicates statistical significance greater than 90% confidence level.

The changes to the land temperature were not considered in these experiments; however, it is highly possible that the long-term influence of CO_2 will also influence the land. Thus modifying the land in a similar way to the removal of oceanCO_2anom could be the next step in the development of this technique.

Regression Analysis. We use the regression model developed by Arblaster et al. (2014). In testing, the Australian-mean October–November Tmax reconstructed by the regression model explains approximately half of the observed variance during 1982–2013 (see Fig. 30.2m of main text).

As noted in the main text, each year's warmth will be determined by a combination of anthropogenic forcing and internal variability, thus, cool seasons such as 2010 can still occur under rising levels of CO_2. Across Australia 2010 was the wettest on record, with an intense La Nina working in concert with warm SSTs associated with extensive rainfall and flooding across Australia, thereby cooling surface temperatures (e.g., Hendon et al. 2014).

Rainfall as a proxy for the heat source of the wave train. The anomalously high rainfall over the central tropical Indian Ocean (15°S–15°N, 60°–80°E; red box in Fig. S30.5a) was used as a proxy for the heat source of the wave train. The influence of IOD was regressed out from this rainfall time series.

REFERENCES

Arblaster, J. M., E.-P. Lim, H. H. Hendon, B. C. Trewin, M. C. Wheeler, G. Liu, and K. Braganza, 2014: Understanding Australia's hottest September on record ["Explaining Extreme Events of 2013 From a Climate Perspective]. *Bull. Amer. Meteor. Soc.,* **95** (9), S37–S41.

Bandoro, J., S. Solomon, A. Donohoe, D. W. J. Thompson, and B. D. Santer, 2014: Influences of the Antarctic ozone hole on Southern Hemispheric summer climate change. *J. Climate*, **27**, 6245–6264, doi:10.1175/JCLI-D-13-00698.1.

Bindoff, N. L., and Coauthors, 2013: Detection and attribution of climate change: From global to regional. *Climate Change 2013: The Physical Science Basis*, T. F. Stocker et al., Eds., Cambridge University Press, 867–952.

Cottrill, A., and Coauthors, 2013: Seasonal forecasting in the Pacific using the coupled model POAMA-2. *Wea. Forecasting*, **28**, 668–680, doi:10.1175/WAF-D-12-00072.1.

Dee, D. P., and Coauthors, 2011: The ERA-Interim reanalysis: Configuration and performance of the data assimilation system. *Quart. J. Roy. Meteor. Soc.*, **137**, 553–597, doi:10.1002/qj.828.

DiNezio, P. N., B. P. Kirtman, A. C. Clement, S.-K. Lee, G. A. Vecchi, and A. Wittenberg, 2012: Mean climate controls on the simulated response of ENSO to increasing greenhouse gases. *J. Climate*, **25**, 7399–7420, doi:10.1175/jcli-d-11-00494.1.

Hendon, H. H., E.-P. Lim, J. Arblaster, and D. L. T. Anderson 2014: Causes and predictability of the record wet spring, Australia 2010. *Climate Dyn.*, **42**, 1155–1174, doi:10.1007/s00382-013-1700-5.

Hudson, D., O. Alves, H. H. Hendon, and G. Wang, 2011: The impact of atmospheric initialisation on seasonal prediction of tropical Pacific SST. *Climate Dyn.*, **36**, 1155–1171, doi:10.1007/s00382-010-0763-9.

Hudson, D., A. G. Marshall, Y. Yin, O. Alves, and H. H. Hendon, 2013: Improving intraseasonal prediction with a new ensemble generation strategy. *Mon. Wea. Rev.*, **141**, 4429–4449, doi:10.1175/MWR-D-13-00059.1.

Hurrell, J. W., J. J. Hack, D. Shea, J. M. Caron, and J. Rosinski, 2008: A new sea surface temperature and sea ice boundary data set for the community atmosphere model. *J. Climate*, **21**, 5145–5153, doi:10.1175/2008JCLI2292.1.

Jones, D. A., W. Wang, and R. Fawcett, 2009: High quality spatial climate data-sets for Australia. *Aust. Meteor. Oceanogr. J.*, **58**, 233–248.

Lim, E.-P., H. H. Hendon, O. Alves, Y. Yin, G. Wang, D. Hudson, M. Zhao, and L. Shi, 2010: Dynamical seasonal prediction of tropical Indo-Pacific SST and Australian rainfall with improved ocean initial conditions. CAWCR Tech. Rep. 032, 26 pp. [Available online at www.cawcr.gov.au/publications/technical-reports/CTR_032.pdf.]

Lim, E.-P., H. H. Hendon, D. L. T. Anderson, and A. Charles, 2011: Dynamical, statistical-dynamical, and multimodel ensemble forecasts of Australian spring season rainfall. *Mon. Wea. Rev.*, **139**, 958–975.

Raupach, M. R., P. R. Briggs, V. Haverd, E. A. King, M. Paget, and C. M. Trudinger, 2009: Australian Water Availability Project (AWAP): CSIRO Marine and Atmospheric Research component: Final report for phase 3. CAWCR Technical Report 013, 67 pp. [Available online at www.cawcr.gov.au/publications/technicalreports/CTR_013.pdf.]

Reynolds, R. W., N. A. Rayner, T. M. Smith, D. C. Stokes, and W. Wang, 2002: An improved in situ and satellite SST analysis for climate. *J. Climate*, **15**, 1609–1625.

Saji, N. H., B. N. Goswami, P. N. Vinayachandran, and T. Yamagata, 1999: A dipole mode in the tropical Indian Ocean. *Nature*, **401**, 360–363.

Son, S.-W., A. Purich, H. H. Hendon, B.-M. Kim, and L. Polvani, 2013: Improved seasonal forecast using ozone hole variability? *Geophys. Res. Lett.*, **40**, 6231–6235, doi:10.1002/2013GL057731.

Yin, Y., O. Alves, and P. Oke, 2011: An ensemble ocean data assimilation system for seasonal prediction. *Mon. Wea. Rev.*, **139**, 786–808, doi:10.1175/2010MWR3419.1.